PAPER

Design of Miniature Implantable Tag Antenna for Radio-Frequency Identification System at 2.45 GHz and Received Power Analysis

HoYu LIN[†a)], ***Student Member***, **Masaharu TAKAHASHI**[††], ***Senior Member***, **Kazuyuki SAITO**[††], ***Member***, ***and*** **Koichi ITO**[†], ***Fellow***

SUMMARY In recent years, there has been rapid developments in radio-frequency identification (RFID) systems, and their industrial applications include logistics management, automatic object identification, access and parking management, etc. Moreover, RFID systems have also been introduced for the management of medical instruments in medical applications to improve the quality of medical services. In recent years, the combination of such a system with a biological monitoring system through permanent implantation in the human body has been suggested to reduce malpractice events and ameliorate the patient suffering. This paper presents an implantable RFID tag antenna design that can match the conjugate impedance of most integrated circuit (IC) chips ($9.3 - j55.2\,\Omega$ at 2.45 GHz. The proposed antenna can be injected into the human body through a biological syringe, owing to its compact size of 9.3 mm × 1.0 mm × 1.0 mm. The input impedance, transmission coefficient, and received power are simulated by a finite element method (FEM). A three-layered phantom is used to confirm antenna performance.

key words: *RFID, in-body wireless communication, implantable tag antenna, human body phantom, received power*

1. Introduction

The radio-frequency identification (RFID) system is one of many wireless communication technologies that has experienced rapid growth in recent years. The advantages of RFID systems have led to their wide application to logistics management, automatic object identification, medicine management, and parking management, etc., because they efficiently reduce human resource requirements and simplify the work process. Furthermore, such systems are now being used to manage medical instruments in medical applications in order to achieve high-quality medical service. In addition, the integration of the RFID system into different wireless technologies, namely, in-body wireless communication, has been suggested because it has the ability to reduce malpractice and ameliorate the quality of life of the patients [1], [2]. The main reason for this suggestion is that the elderly population has increased in recent years in developed countries which, as a result, are facing mounting healthcare problems. On the other hand, the chronic undersupply of healthcare workers has spawned medical errors and degraded medical service quality; therefore, the introduction of such an integrated system can reduce the pressure on the already overburdened healthcare system. Hence, an integrated RFID system with an in-body wireless communication is very attractive.

In addition to in-body wireless communication, one of the body-area-network (BAN) protocols [3], [4] is also involved. For several years during the 1980s, in-body wireless communication was developed for use in medical applications, particularly for the implantation of a cardiac pacemaker into the human body to regulate the human heart rate via asystolic control, which causes ventricular contraction. With the ongoing development of modern technologies, wireless communication with implantable devices has become a reality because of the use of implantable integrated circuits (ICs), sensors, batteries, antennas, etc., for example, in capsule endoscopy [5] and animal chip implants [6]. However, the complex human body causes extreme attenuation of the antenna performance; therefore, some of the essentials of antenna design should be completely reconsidered: (a) the physical antenna size should be miniaturized such that the antenna can be injected into the human body via a syringe in order to reduce pain during injection, and (b) the antenna should be coated with a biological material to avoid direct contact with the human tissues and reduce attenuation from the human body.

Some recent papers have addressed these issues; for instance, the planar inverted-F antenna (PIFA)-like structure on a substrate with high dielectric loss and a cavity slot antenna design was proposed [7]–[10] in order to reduce the antenna size. RF transmission between the antenna and the human body has been discussed in [11]–[13].

In this paper, we begin by proposing a compact implantable tag antenna that is designed in combination with an IC chip to function as a passive tag device. The conjugate impedance of the IC chip is $9.3 - j55.2\,\Omega$ at 2.45 GHz [14]; that is, the input impedance of the antenna should be designed to be $9.3 + j55.2\,\Omega$ for impedance matching. The proposed antenna has a miniaturized size of 9.1 mm × 0.8 mm × 0.8 mm owing to the folded structure [15], and the size is 9.3 mm × 1.0 mm × 1.0 mm after glass coating. The performance of the proposed antenna is investigated by simulating its impedance characteristic, transmission coefficient, and received power by using a finite element method (FEM). Furthermore, a three-layered phantom is introduced into the simulation and measured as a substitute for a real human arm [16].

Manuscript received July 11, 2013.
Manuscript revised September 9, 2013.

[†]The authors are with the Graduate School of Engineering, Chiba University, Chiba-shi, 263-8522 Japan.
[††]The authors are with Research Center for Frontier Medical Engineering, Chiba University, Chiba-shi, 263-8522 Japan.
a) E-mail: hoyu_lin@graduate.chiba-u.jp

DOI: 10.1587/transcom.E97.B.129

The remainder of this paper is organized as follows. Section 2 describes the antenna structure and simulation model. Section 3 shows and discusses the simulation and measurement results of the antenna impedance characteristic. In Sect. 4, the link budget of the received power between the proposed antenna and the circularly polarized (CP) antenna is discussed. The conclusions of this study are presented in Sect. 5.

2. Antenna Structure and Simulation Model

The geometry of the proposed antenna is shown in Fig. 1. The antenna is fabricated by bending a narrow strip of 0.1 mm into a folded structure to reduce the physical size. Both the width and the height of the proposed antenna are 0.8 mm. Thus, the total size of the proposed antenna is 9.1 mm × 0.8 mm × 0.8 mm. Moreover, the loop structure is placed near the feeding point to match the conjugate impedance of the IC chip ($9.3 - j55.2\,\Omega$ at 2.45 GHz). The size of the loop structure is 6.2 mm (L_1)× 0.35 mm (W_1). Finally, the proposed antenna is 9.3 mm × 1.0 mm × 1.0 mm after coating with glass ($\varepsilon_r = 5.0$).

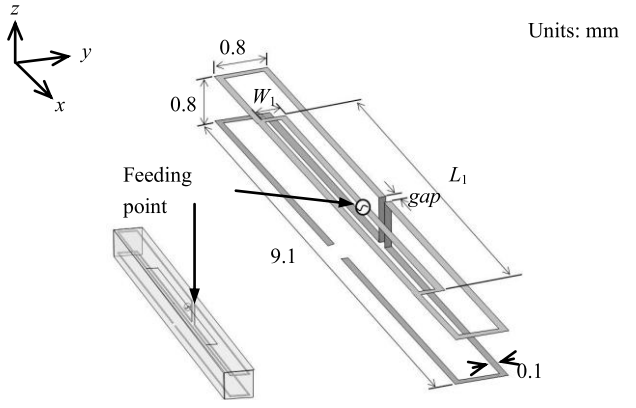

Fig. 1 Antenna geometry and glass coating.

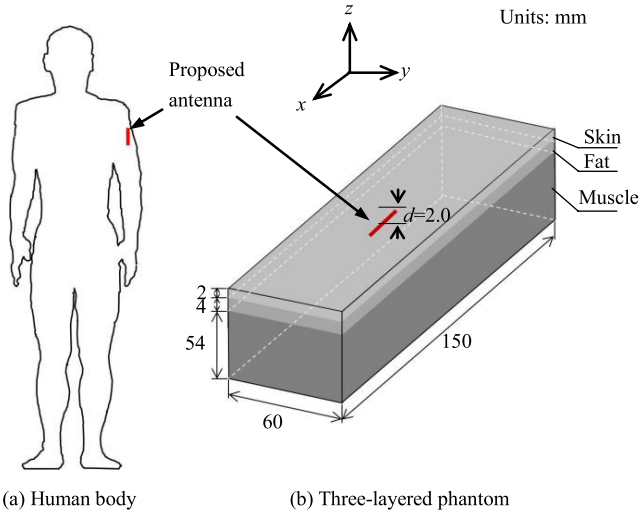

(a) Human body (b) Three-layered phantom

Fig. 2 Simulation model.

We have modeled the implantable antenna and glass coating using FEM with the aim of obtaining accurate results while maintaining a reasonable computational complexity. Moreover, we evaluated the antenna performance with a real human body, as shown in Fig. 2(a). In this case, we modeled a three-layered human phantom as a substitute for the human arm, as shown in Fig. 2(b). The human phantom was constructed with skin ($\varepsilon_r = 38.0$, $\sigma = 1.5$ S/m), fat ($\varepsilon_r = 5.3$ $\sigma = 0.1$ S/m), and muscle ($\varepsilon_r = 52.7$, $\sigma = 1.7$ S/m) at the desired frequency of 2.45 GHz [17] with thicknesses of 2 mm, 4 mm, and 54 mm, respectively. The size of the phantom was 150 mm × 60 mm × 60 mm. In addition, we have embedded the proposed antenna in the fat layer at a depth of 2 mm because the loss in fat is less than that in skin and muscle.

3. Impedance Characteristics and Measurements

3.1 Impedance Characteristics without the Loop Structure

In this section, we discuss the impedance characteristics when the dipole antenna is bent into a folded structure. Figures 3(a) and (b) show the current distributions on the dipole antenna and folded antenna, respectively. The total length (L_{total}) of both antennas is 40.3 mm. We observe from Fig. 3(b) that the folded antenna has a width of 0.8 mm ($w \ll \lambda$) between the folds, and four currents I_a, I_b, I_c, and I_d pass through the antenna. Table 1 summarizes the simulation results when the dipole antenna is bent as a folded structure. According to these results, it is found that the

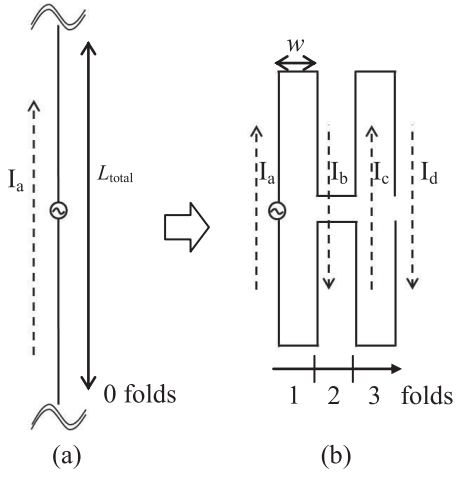

Fig. 3 Current distribution on the proposed antenna.

Table 1 Comparison of the impedance characteristics of the different folds at 2.45 GHz.

Folds	Resistance [Ω]	Reactance [Ω]
0	408.5	-163.3
1	96.5	334.5
2	25.9	130.5
3	18.0	57.9

four currents are mutually cancelled; therefore, the resistance is reduced from 408.5 Ω to 18 Ω. Moreover, the inductive impedance is reduced by increasing the capacitive coupling, which is provided by the folded structure. Therefore, the reactance changes from −163.3 Ω to 57.9 Ω.

3.2 Impedance Characteristics with the Loop Structure and Experimental Results

Adding a loop structure near the feeding point improves the input impedance of the proposed antenna to match the conjugate impedance of 9.3 − *j*55.2 Ω. The main reason is that the currents on the proposed antenna are cancelled mutually, therefore the resistance of the proposed antenna can be reduced [18]. The effect of the loop structure on the antenna impedance is investigated by varying the parameters L_1, W_1, and *gap*. The simulated results are shown in Figs. 4(a)–(c) for these parameters. In Fig. 4(a), it is found that when L_1 changes from 5.2 mm to 7.2 mm, the resistance increases from 6.4 Ω to 14 Ω; however, the reactance does not change. In Fig. 4(b), W_1 is a key factor for impedance matching; when W_1 varies from 0.15 mm to 0.55 mm, it not only causes an increase in the resistance but also has a stronger impact on the reactance. Therefore, good impedance matching can be obtained when W_1 is equal to 0.35 mm. Figure 4(c) shows that the parameter *gap* has an influence on the impedance matching; thus, good impedance matching is achieved when *gap* is equal to 0.2 mm.

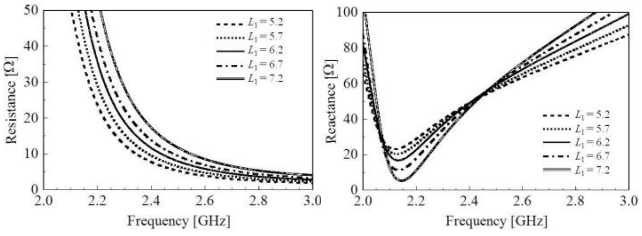

(a) Parameter L_1 (W_1 = 0.35, *gap* = 0.2)

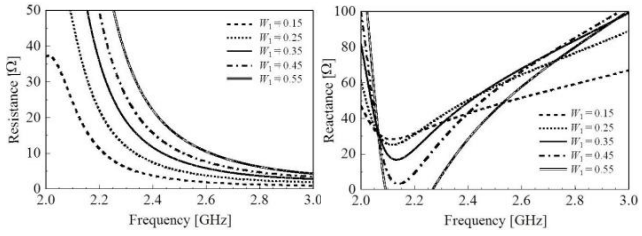

(b) Parameter W_1 (L_1 = 6.2, *gap* = 0.2)

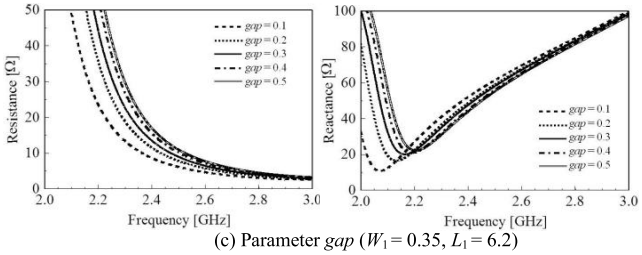

(c) Parameter *gap* (W_1 = 0.35, L_1 = 6.2)

Fig. 4 Simulated results for L_1, W_1, and *gap* for impedance matching.

As per the above discussion, the loop structure can apparently improve the input impedance of the proposed antenna from 18.0 + *j*57.9 Ω to 9.5 + *j*54.1 Ω, which approaches the conjugate impedance of 9.3 − *j*55.2 Ω, as shown in Fig. 5(a). Figure 5(b) shows a comparison of the simulated and measured input impedances. As a result, the measured impedance of 9.1 + *j*47.4 Ω shows good agreement with the simulated one. However, the measured results appear to be flat, which is caused by the lossy phantom that surrounds the proposed antenna and 1/4-wavelength balun. Figures 6(a) and (b) show the fabricated antenna, which is connected by 1/4-wavelength balun (with a length of 30.6 mm at 2.45 GHz) and a three-layered human phantom, respectively. The measurement setup for testing the input impedance of the proposed antenna is shown in Fig. 6(c). In our experiment, a hole is dug into the phantom to connect the balun to the antenna and fix the antenna in the fat layer of the three-layered phantom.

In this study, an N5230C network analyzer and the dielectric probe kit 85070E (Agilent Tech., CA) are used for the dielectric measurements, and the measurements of the three-layered phantom are obtained at 2.45 GHz. Table 2 summarizes the comparison between the target and the measured permittivity and conductivity of the three-layered phantom with those of the reference skin, fat, and muscle [17]. All measured results are below or approaching 5% when compared with the target values, and this small difference has no influence on the antenna performance [19]. Table 3 lists the compositions of the skin, fat, and muscle.

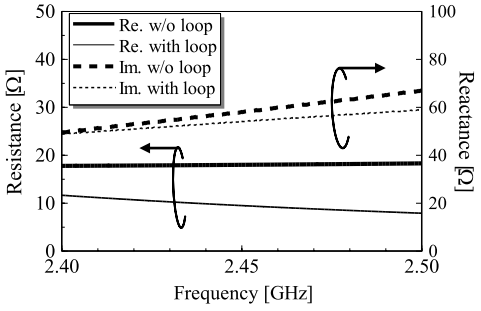

(a) With and without the loop structure

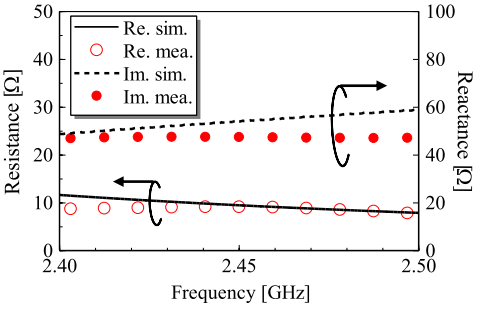

(b) Simulation and measured results

Fig. 5 Impedance characteristics of the proposed antenna.

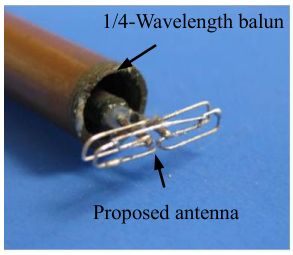

(a) Fabricated antenna

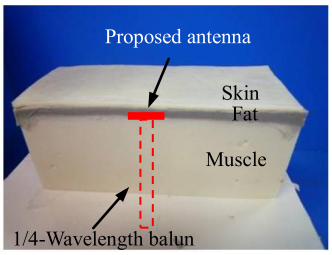

(b) Three-layered phantom

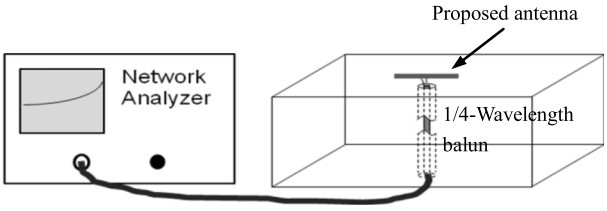

(c) Measurement setup

Fig. 6 Measurement of the impedance characteristics.

Table 2 Electric constants of the test phantom at 2.45 GHz.

	Permittivity			Conductivity [S/m]		
Tissues	Target	Meas.	%	Target	Meas.	%
Skin	38.0	41.1	8.9	1.5	1.4	6.6
Fat	5.3	5.2	1.8	0.1	0.1	0
Muscle	52.7	55.2	4.6	1.7	1.6	6.1

Table 3 Composition of the three-layered phantom.

Materials	Human Tissues (%)		
	Skin	Fat	Muscle
Deionized Water	18.4		86.2
Sodium dehydroacetate			0.05
TX-151			2.1
NaCl			0.25
Polyethylene powder			8.7
Agar			2.7
Silicon		64.5	
Glycerin		22.6	
Gelatin	10		
Silicone emulsion	71.6		
Aluminum powder		12.9	

4. Path Loss

Estimation of the path loss between an external reader/writer (R/W) and a tag is essential because the tag is embedded in the human body, which is a complex environment. Therefore, parameter analysis is performed by using a high-frequency structure simulator (HFSS) (v. 10.1, Ansoft Corp.). The transmission coefficient and received power are analyzed and discussed in detail in Sects. 4.1 and 4.2, respectively. In addition, the reliability of the calculated received power is confirmed upon completion of the experiment.

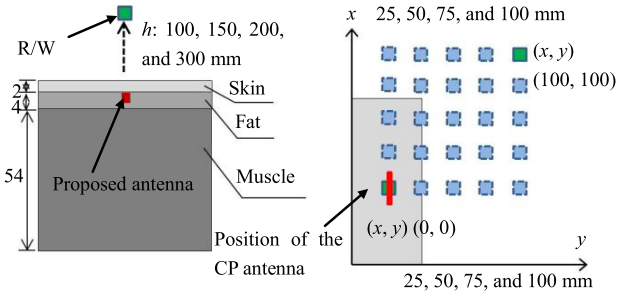

(a) Simulation model for the transmission coefficient

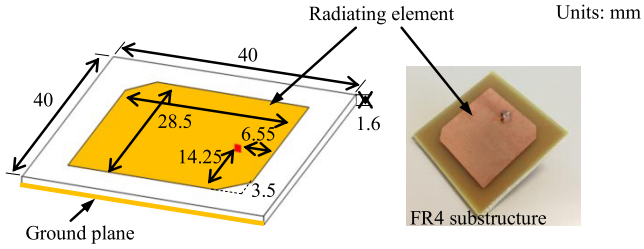

(b) R/W (circularly polarized antenna)

Fig. 7 Simulation model and CP antenna geometry.

4.1 Transmission Coefficient

Figures 7(a) and (b) show the simulation model and geometry of the CP antenna. As shown in Fig. 7(a), the proposed antenna is in the fat layer of the three-layered phantom, and the CP antenna is set above the phantom at a specific height (h).

The reactive near-field distance (r) can be calculated by using the following formula:

$$r = \frac{\lambda}{2\pi} \tag{1}$$

Thus, r = 19.4 mm is obtained using (1) at 2.45 GHz of the ISM band (λ = 0.122 m). We assumed the antenna is work in the region between the reactive near-field and far-field, so the separation between the antennas should be larger than r. Accordingly, the CP antenna is located at h = 25–300 mm from the proposed antenna. Figure 7(a) shows that the position of the CP antenna is varied from (x, y) (0 mm, 0 mm) to (100 mm, 100 mm) in order to achieve a significant correlation of the transmission coefficient between the proposed antenna and the CP antenna. Figure 7(b) shows the geometry of the CP antenna fabricated on a flame retardant type 4 substrate (ε_r = 4.4). The size of the CP antenna is 40 mm × 40 mm × 1.6 mm. The maximum antenna gain and bandwidth (< 3-dB axial ratio) are 2.9 dBi and 28 MHz, respectively.

Figures 8(a)–(d) show the simulated transmission coefficients of the proposed antenna in the phantom. It can be

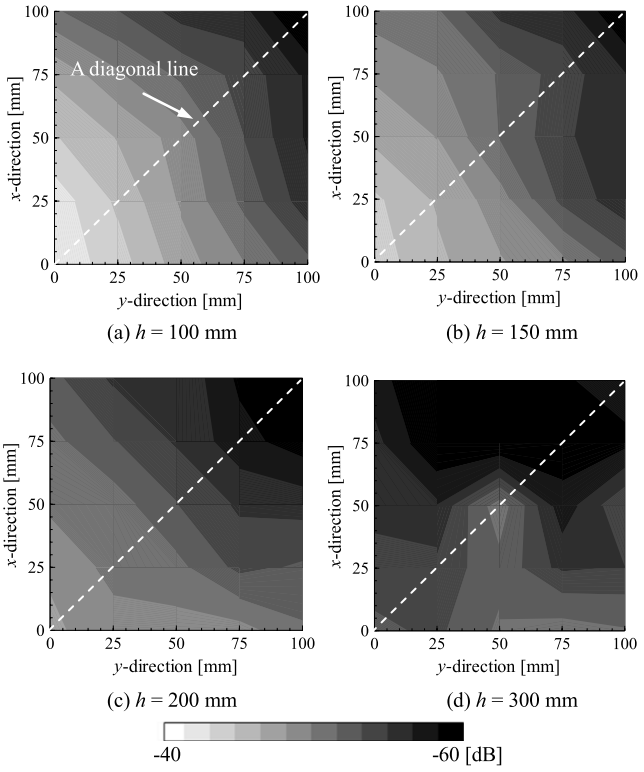

Fig. 8 Simulation results for the transmission coefficient for various positions of the CP antenna h.

observed from Figs. 8(a) and (b) that the results are symmetric in these figures according to a diagonal line, which might be due to the proximity of the CP antenna to the proposed antenna. Moreover, the strength of the transmission coefficient in the x-direction is higher than that in the y-direction, because the electromagnetic wave is affected by the edge of the phantom. As shown in Figs. 8(c) and (d), the transmission coefficient becomes weak as h increases. Moreover, we also find that the nonsymmetrical structure of the phantom causes a change in the electromagnetic wave in the x- and y-directions.

As per the above discussion, the electromagnetic wave of the proposed antenna depends on the phantom structure. However, there is less influence from the phantom on the transmission coefficient of the proposed antenna when there is a small distance between the proposed antenna and the CP antenna. In addition, the three-layered phantom can be considered the most worthy candidate for in-body wireless communication. This implies that the antenna can work well in other models that are close to the structure of a real human arm [16].

4.2 Link Budget and Measurement

In the RFID system, the link budget is generally used for estimating the amount of power that is actually received by a tag placed at a distance r from the isotropic antenna, which is denoted as the power required for R/W. A minimum RF input power of 10 μW to 50 μW (−20 dBm to −13 dBm) is

Table 4 Parameters of the link budget at 2.45 GHz.

R/W antenna (CP antenna)	
R/W input power: P_{R} [W]	1.0
R/W antenna gain: G_{R} [dBi]	2.9
EIRP of the R/W: P_{ERIP} [W]	1.958
Losses in cable and connector: P_{CL} [dB]	-3.0
Tag antenna (implantable RFID antenna)	
Tag antenna gain: G_{T} [dBi]	-18.8
Max. practical value of input resistance: R_{c} [Ω]	9.3
Distance : h [mm]	100
Polarization mismatch loss: P_{PL} [dB]	-3.0
Received voltage: V_{Tag} [V]	0.047
Received power of tag: P_{Tag} [dBm]	-12.1

required to power up the chip [20]. According to the link budget, the received power of the proposed antenna is calculated with the following formulas:

$$V_{Tag} = \frac{\lambda}{4\pi h}\sqrt{P_R G_R G_T R_c}, \text{ and} \tag{2}$$

$$P_{Tag} = \frac{V_{Tag}^2}{R_c}. \tag{3}$$

In this case, we assume a lossless environment and matched antennas, where λ is the wavelength in free space, P_{R} is the transmitted power by the reader, and P_{Tag} is the received power of the tag's IC chip. G_{R} and G_{T} are the gains in the reader and tag, respectively. The load impedance R_{c} is 9.3 Ω which represents the input resistance of the IC chip. In addition, the losses in the coaxial cable and connector for R/W should be considered (the typical loss in the antenna cables is ∼2.5 dB) [21]. Further, the polarization mismatch between the antennas with different polarizations, namely, circular polarization and vertical (horizontal) polarization, must be considered, and Eq. (3) should be revised as

$$P_{Tag} = 10\log\left(\frac{V_{Tag}^2}{R_c}\right) + P_{CL} + P_{PL}, \tag{4}$$

where P_{CL} expresses the losses of the coaxial cable and connector, and P_{PL} is the polarization mismatch. Both of these quantities are set to 3 dB in theory. Therefore, we can validate of the measured received power using Eq. (4). These parameters are summarized in Table 4. As summarized in Table 4, the received power of the proposed antenna is −12.1 dBm when the CP antenna is located at h = 100 mm.

Figure 9 shows the measurement setup for the received power. Port1 and Port2 of the network analyzer connect to the proposed antenna and CP antenna, respectively; a fixed antenna support is used to change the height of the CP antenna. Besides, the measured gains of the proposed antenna and CP antenna are −19.3 and 2.2 dBi, respectively.

The received power is obtained generally by calculating the measured S_{21} and accepted power of the CP antenna. However, we measure the received power of the proposed

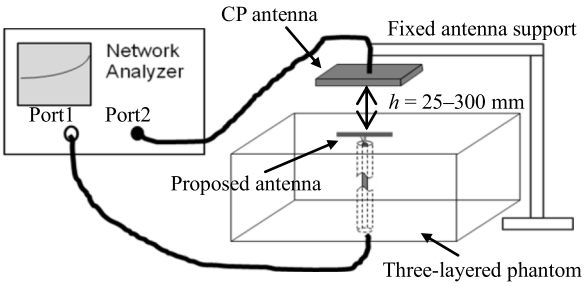

Fig. 9 Measurement setup for the received power.

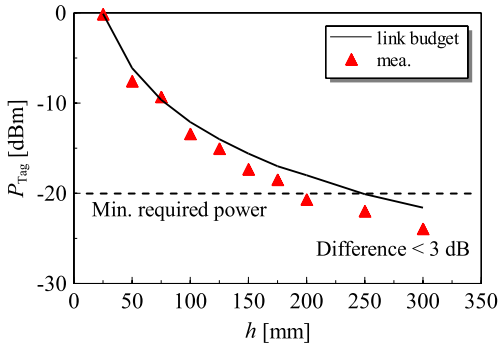

Fig. 10 Received power comparison between the link budget and the measurement result when the CP antenna is placed above the three-layered phantom at h = 25–300 mm with position (x, y) = (0 mm, 0 mm) fixed.

antenna before, there are two points should be noted: (a) Since the proposed antenna has a conjugate impedance that is different from 50 Ω system of network analyzer (NA), the mismatch between them is necessary to be considered when we measure S_{21}. (b) The input impedance of the proposed antenna is 9.5 + j54.1 Ω close to 9.3 + j55.2 Ω values of the conjugate match with the IC. However, fabrication error in antenna often causes a subtle difference between the measured impedance of 9.1 + j47.4 Ω and simulated result of 9.5 + j54.1 Ω. Therefore, when the (a) mismatch loss and (b) fabrication error are considered, we could ensure that the measured result of S_{21} is accurate and reliable. According to this concept, the received power of the proposed antenna can be obtained as follows. For instance, if S_{21} is −10 dB which includes the mismatch loss and fabrication error, then if 30 dBm (1 Watt) is delivered from CP antenna to the proposed antenna, then 20 dBm power is received at the proposed antenna.

Figure 10 shows the comparison of the calculated received power by using the link budget and the measured received power when the CP antenna is located at h = 25–300 mm; however, the antenna position is fixed at (0, 0). As a result, it is found that when the CP antenna is placed at h = 25–195 mm, the measured received power can satisfy the minimum required power of −20 dBm. Moreover, the measured results agree with the calculations because the difference is less than 3 dB.

5. Conclusions

An implantable tag antenna with an IC chip for an RFID system is proposed in this paper. In the proposed antenna, a conjugated impedance of 9.3 − j55.2 Ω is well-matched by adding a loop structure in the human phantom. Moreover, the measured input impedance agrees well with the simulated impedance. The received power satisfies the required power of −20 dBm when the CP antenna is located at h = 25–195 mm. In addition, the reliability of the received power is confirmed, because the difference is less than 3 dB. The proposed antenna has a compact size of 9.3 mm × 1.0 mm × 1.0 mm such that it can be easily injected into the human body by using a syringe. In our future work, an animal experiment will be carried out to demonstrate wireless communication between the proposed antenna and an R/W.

Acknowledgments

This work was supported by a Grant-in-Aid for Scientific Research(C) 21560384.

References

[1] A. Sani, M. Rajab, R. Foster, and Y. Hao, "Antennas and propagation of implanted RFIDs for pervasive healthcare applications," Proc. IEEE, vol.98, no.9, pp.1648–1655, Sept. 2010.
[2] P. Rotter, B. Daskala, and R. Compano, "RFID implants: Opportunities and and challenges for identifying people," IEEE Tochnnlogy and Society Magazine, vol.27, no.2, pp.24–32, 2010.
[3] P.S. Hall and Y. Hao, "Antennas and propagation for body centric communications," Proc. European Conference on Antenna and Propagation (EuCAP 2006).
[4] B.M. Steinhaus, R.E. Smith, and P. Crosby, "The role of t elecommunications in future implantable device systems," in Proc. IEEE Conf. Medicine and Biology, vol.2, pp.1013–1014, Nov. 1994.
[5] T. Kumagai, K. Saito, M. Takahashi, and K. Ito, "A small 915MHz receiving antenna for wireless power transmission aimed at medical applications," Int. J. Technology (IJTech), vol.2, issue 1, pp.20–27, Jan 2011.
[6] [Online] Available: http://www.positiveidcorp.com/
[7] J. Kim and Y. Rahmat-Samii, "Implanted antennas inside a human body: Simulations, designs, and characterizations," IEEE Trans. Microw. Theory Tech., vol.52, no.8, pp.1934–1943, Aug. 2004.
[8] F.-J. Huang, C.-M. Lee, C.-L. Chang, L.-K. Chen, T.-C. Yo, and C.-H. Luo, "Rectenna application of miniaturized implantable antenna design for triple-band biotelemetry communication," IEEE Trans. Antennas Propag., vol.59, pp.2646–2653, July 2011.
[9] A. Kiourti and K.S. Nikita, "Miniature scalp-implantable antennas for telemetryin the MICS and ISM bands: Design, safety considerations and link budget analysis," IEEE Trans. Antennas Propag., vol.60, no.8, pp.3568–3575, Aug. 2012.
[10] W. Xia, K. Saito, M. Takahashi, and K. Ito, "Performances of an implanted cavity slot antenna embedded in the human arm," IEEE Trans. Antennas Propag., vol.57, no.4, pp.894–899, April 2009.
[11] Z.N. Chen, G.C. Liu, and T.S.P. See, "Transmisson of RF signals between MICS loop antennas in free space and implanted in the human head," IEEE Trans. Antennas Propag., vol.57, no.6, pp.1850–1853, June 2009.
[12] W.G. Scanlon, J.B. Burns, and N.E. Evans, "Radiowave propagation from a tissue-implanted source at 418 MHz and 916.5 MHz," IEEE Trans. Biomed. Eng., vol.47, no.4, pp.527–534, April 2000.

[13] T.S.P. See, X. Qing, Z.N. Chen, C.K. Goh, and T.M. Chiam, "RF transmission in/through the human body at 915 MHz," Antennas and Propagation Society International symposium (SPSURSI), pp.1–4, April 2010.
[14] M. Usami and M. Ohki, "The μ-chip: An ultra-small 2.45 GHz RFID chip for ubiquitous recognition applications," IEICE Trans. Electron., vol.E86-C, no.4, pp.521–528, April 2003.
[15] H.Y. Lin, M. Takahashi, K. Saito, and K. Ito, "Design of small implantable RFID antenna for 2.4 GHz for in-body wireless communication," IEICE Commun. Express, vol.2, no.2, pp.31–35, Feb. 2013.
[16] H.Y. Lin, M. Takahashi, K. Saito, and K. Ito, "Performances of implantable folded dipole antenna for in-body wireless communication," IEEE Trans. Antennas Propag., vol.61, no.3, pp.1363–1370, March 2013.
[17] Dielectric Properties of Body Tissues (IFAC), http://niremf.ifac.cnr.it/tissprop/
[18] G. Marrocco, "The art of UHF RFID antenna design: Impedance-matching and size-reduction techniques," IEEE Antennas Propag. Mag., vol.50, no.1, pp.66–79, Feb. 2008.
[19] K. Ito, "Human body phantoms for evaluation of wearable and implantable antennas," Antennas and Propagation, (EuCAP 2007), pp.1–6, 2007.
[20] L. Harvey, "RFID design principles, second edition," Feb. 2012, ch. 5.
[21] L. Harvey, "RFID design principles, second edition," Feb. 2012, ch. 6.

HoYu Lin was born in Taipei, Taiwan, in April 1983. He received the B.S. and M.E. degree in electronic engineering from Southern Taiwan University, Tainan, Taiwan, in 2007 and 2009, respectively, where he is currently pursuing the D.E. degree at Chiba University, Chiba, Japan. His main interests have been electrically antennas for wireless local area network, radio frequency identification, and the development and design of the antenna for implantable devices by use of numerical and experimental phantoms. Mr. Lin is a member of the Institute of Electronics, Information and Communication Engineers (IEICE), Japan.

Masaharu Takahashi (M'95–SM'02) was born in Chiba, Japan, in December 1965. He received the B.E. degree in electrical engineering from Tohoku University, Miyagi, Japan, in 1989, and the M.E. and D.E. degrees in electrical engineering from the Tokyo Institute of Technology, Tokyo, Japan, in 1991 and 1994, respectively. From 1994 to 1996, he was a Research Associate, and from 1996 to 2000, an Assistant Professor with the Musashi Institute of Technology, Tokyo, Japan. From 2000 to 2004, he was an Associate Professor with the Tokyo University of Agriculture and Technology, Tokyo, Japan. He is currently an Associate Professor with the Research Center for Frontier Medical Engineering, Chiba University, Chiba, Japan. His main interests are electrically small antennas, planar array antennas, and EM compatibility. Dr. Takahashi is a Senior Member of the Institute of Electronics, Information and Communication Engineers (IEICE), Japan. He was the recipient of the 1994 IEEE Antennas and Propagation Society (IEEE AP-S) Tokyo Chapter Young Engineer Award.

Kazuyuki Saito (S'99–M'01) was born in Nagano, Japan, in May 1973. He received the B.E., M.E., and D.E. degrees in electronic engineering from Chiba University, Chiba, Japan, in 1996, 1998 and 2001, respectively. He is currently an Associate Professor with the Research Center for Frontier Medical Engineering, Chiba University. His main interest is in the area of medical applications of microwaves including microwave hyperthermia. Dr. Saito is a member of the Institute of Electrical, Information and Communication Engineers (IEICE), Japan, the Institute of Image Information and Television Engineers of Japan (ITE), and the Japanese Society for Thermal Medicine. He was the recipient of the IEICE Antennas and Propagation Society (AP-S) Freshman Award, the Award for Young Scientist of the URSI General Assembly, the IEEE AP-S Japan Chapter Young Engineer Award, the Young Researchers' Award of the IEICE, and the International Symposium on Antennas and Propagation (ISAP) Paper Award in 1997, 1999, 2000, 2004, and 2005 respectively.

Koichi Ito (M'81–SM'02–F'05) received the B.S. and M.S. degrees from Chiba University, Chiba, Japan, in 1974 and 1976, respectively, and the D.E. degree from the Tokyo Institute of Technology, Tokyo, Japan, in 1985, all in electrical engineering. From 1976 to 1979, he was a Research Associate with the Tokyo Institute of Technology. From 1979 to 1989, he was a Research Associate with Chiba University. From 1989 to 1997, he was an Associate Professor with the Department of Electrical and Electronics Engineering, Chiba University, and is currently a Professor with the Department of Medical System Engineering, Chiba University. From 2005 to 2009, he was Deputy Vice-President for Research, Chiba University. From 2008 to 2009, he was Vice-Dean of the Graduate School of Engineering, Chiba University. Since April 2009, he has been the Director of the Research Center for Frontier Medical Engineering, Chiba University. In 1989, 1994, and 1998, he visited the University of Rennes I, Rennes, France, as an Invited Professor. His main research interests include analysis and design of printed antennas and small antennas for mobile communications, research on evaluation of the interaction between EM fields and the human body by use of numerical and experimental phantoms, microwave antennas for medical applications such as cancer treatment, and antennas for body-centric wireless communications. Dr. Ito is a Fellow of the Institute of Electronics, Information and Communication Engineers (IEICE), Japan. He is a member of the American Association for the Advancement of Science, the Bioelectromagnetics Society (BEMS), the Institute of Image Information and Television Engineers of Japan (ITE), and the Japanese Society for Thermal Medicine. Hewas chair of the Technical Group on Radio and Optical Transmissions, ITE from 1997 to 2001, chair of the Technical Committee on Human Phantoms for Electromagnetics, IEICE from 1998 to 2006, chair of the IEEE Antennas and Propagation (AP-S) Japan Chapter from 2001 to 2002, Technical Program Committee (TPC) co-chair of the 2006 IEEE International Workshop on Antenna Technology (iWAT2006), vice-chair of the 2007 International Symposium on Antennas and Propagation (ISAP2007), general chair of iWAT2008, co-chair of ISAP2008, and an Administrative Committee (AdCom) member for the IEEE AP-S from 2007 to 2009. He currently serves as an associate editor for the IEEE TRANSACTIONS ON ANTENNAS AND PROPAGATION. He is a Distinguished Lecturer for the IEEE AP-S, and chair of the Technical Committee on Antennas and Propagation, IEICE. He has been appointed as general chair of ISAP2012, Nagoya, Japan, 2012, and a member of the Board of Directors, BEMS, and a Councilor to the Asian Society of Hyperthermic Oncology (ASHO). He has been appointed as General Chair of ISAP2012 to be held in Nagoya, Japan, and as a member the IEEE Life Sciences New Initiative (LSNI) Project Team. He has been elected as a delegate to the European Association on Antennas and Propagation (EurAAP).